Biogeosciences Discuss., 9, 13817–13856, 2012
www.biogeosciences-discuss.net/9/13817/2012/
doi:10.5194/bgd-9-13817-2012

Biogeosciences Discussions

Kinetic bottlenecks to chemical exchange rates for deep-sea animals – Part 1: Oxygen

A. F. Hofmann[1,*], **E. T. Peltzer**[1], **and P. G. Brewer**[1]

[1]Monterey Bay Aquarium Research Institute (MBARI), 7700 Sandholdt Road, Moss Landing, CA 95039–9644, USA
[*]now at: German Aerospace Center (DLR), Institute of Technical Thermodynamics, Pfaffenwaldring 38–40, 70569 Stuttgart, Germany

Received: 9 September 2012 – Accepted: 3 October 2012 – Published: 11 October 2012

Correspondence to: A. F. Hofmann (ahofmann.mbari@gmail.com)

Published by Copernicus Publications on behalf of the European Geosciences Union.

Abstract

Ocean warming will reduce dissolved oxygen concentrations which can pose challenges to marine life. Oxygen limits are traditionally reported simply as a static concentration thresholds with no temperature, pressure or flow rate dependency. Here we treat the oceanic oxygen supply potential for heterotrophic consumption as a dynamic molecular exchange problem analogous to familiar gas exchange processes at the sea surface. A combination of the purely physico-chemical oceanic properties temperature, hydrostatic pressure, and oxygen concentration defines the ability of the ocean to supply oxygen to any given animal. This general oceanic oxygen supply potential is modulated by animal specific properties such as the diffusive boundary layer thickness to define and limit maximal oxygen supply rates. Here we combine all these properties into formal, mechanistic equations defining novel oceanic properties that subsume various relevant classical oceanographic parameters to better visualize, map, comprehend, and predict the impact of ocean deoxygenation on aerobic life. By explicitly including temperature and hydrostatic pressure into our quantities, various ocean regions ranging from the cold deep-sea to warm, coastal seas can be compared. We define purely physico-chemical quantities to describe the oceanic oxygen supply potential, but also quantities that contain organism-specific properties which in a most generalized way describe general concepts and dependencies. We apply these novel quantities to example oceanic profiles around the world and find that temperature and pressure dependencies of diffusion and partial pressure create zones of greatest physical constriction on oxygen supply typically at around 1000 m depth, which coincides with oxygen concentration minimum zones. In these zones, which comprise the bulk of the world ocean, ocean warming and deoxygenation have a clear negative effect for aerobic life. In some shallow and warm waters the enhanced diffusion and higher partial pressure due to higher temperatures might slightly overcompensate for oxygen concentration decreases due to decreases in solubility.

BGD

9, 13817–13856, 2012

1 Introduction

One of the challenges facing ocean science is the need to make a formal connection between the emerging changes in the physico-chemical properties of the ocean such as rising temperature and CO_2 levels, declining O_2, and the responses of marine animals. Here, we focus on the theoretical background for characterization, description, and mapping of the impacts of ocean deoxygenation from a kinetic perspective.

The kinetics of diffusive processes are well understood and embodied in Fick's first Law. The solubility of the metabolically important gases is well known as a function of salinity and temperature (Weiss, 1970, 1974; Garcia and Gordon, 1992). From this and the observed distributions, partial pressures – the essential diffusive quantity across membranes – can be deduced. Likewise, the diffusion coefficients of the substances in question and their variation with temperature, boundary layer thickness and fluid flow are known. From these fundamental principles and observations, one can derive additional parameters which embodied the fundamental chemistry and physics in useful ways to illustrate and predict future changes in the ocean.

The problem of setting limits for aerobic respiration has been traditionally defined as a series of simple oxygen concentration limits. For example coastal ocean "dead zones" are usually defined as having less than $2\,mg\,O_2\,l^{-1}$ ($61\,\mu mol\,O_2\,kg^{-1}$) and "suboxic" conditions as less than $10\,\mu mol\,O_2\,kg^{-1}$. The term "hypoxia" is used to describe a rather wide range of values; for example very large areas of the ocean are predicted to become hypoxic under climate warming (Shaffer et al., 2009) based upon a concentration threshold of of $80\,\mu mol\,O_2\,kg^{-1}$ as defined in Gray et al. (2002). In a major series of coordinated papers reviewing the conditions for hypoxia (Middelburg and Levin, 2009; Gooday et al., 2009; Levin et al., 2009; Kemp et al., 2009; Zhang et al., 2010; Ekau et al., 2010; Rabalais et al., 2010; Pena et al., 2010; Naqvi et al., 2010; Gilbert et al., 2010) simple concentration limits were again cited.

A definition based simply upon concentration has served us well for decades in describing a steady state ocean since it provides a reasonable approximation to the O_2

BGD
9, 13817–13856, 2012

resource available at a particular site. But it is ill suited to a comparison of ocean regions of different temperatures and pressures, or for an ocean undergoing climate change, since essential temperature, pressure, diffusivity and related factors are not included. This concept of kinetic limitation is not new to marine biologists; for example, Lazier and Mann (1989) and Karp-Boss et al. (1996) have looked at the process for specific organisms. In this paper, we consider only the general case and derive a set of quantities that better describe the kinetic limits on the oxygen supply potential of the ocean for animal respiration than does a simple oxygen concentration value.

The intention is to combine the essential physico-chemical oceanic properties in a mechanistically meaningful, yet generically applicable way. We define quantities that include only the organism-independent physical properties and that can be used to describe, map, and compare various oceanic regions of interest with respect to their oxygen supply potential. Secondarily, we define quantities that do include some organism-specific properties e.g. the respiratory surface diffusive boundary layer thickness and the oxygen partial pressure in direct contact with the animal respiratory tissue surface (essentially venous blood pO_2); but we do so only to illustrate the general principles and dependencies, and to investigate the potential for change of purely physical properties under ocean warming and oxygen depletion scenarios. Scientists concerned with particular species of animals can then apply these formulae for specific cases.

The quantities we define here are meant to be used in physico-chemical models of the ocean, for mapping the O_2 supply capacity of areas of interest such as in climate change assessments or for inter-regional comparisons to assist in ecosystem based management decisions as in the designation and knowledge of marine protected areas (e.g. Palumbi et al., 2009; Tallis et al., 2012).

2 Oceanic oxygen supply: physico-chemical vs. organism specific quantities

The O_2 demands of marine organisms have classically been described by physiologists as a rate problem (e.g. Hughes, 1966) in which diffusive transport across a boundary

BGD
9, 13817–13856, 2012

layer driven by partial pressure differences takes place; and, as in knowledge of gas exchange rates at the sea surface (e.g. Wanninkhof, 1992) where wind speed is a critical variable, bulk fluid flow velocity is important. A simple concentration value alone cannot adequately describe this process. For example, giving a concentration as a limit provides no temperature dependent information, so that the same value is assumed to be limiting over a temperature span of possibly 30 °C. This can be overcome to some extent by providing pO_2 as a limiting value (Hofmann et al., 2011), but the rate problem for gas transfer across a diffusive boundary layer contains also terms for diffusivity, and the relationship between boundary layer thickness and velocity over the surface, and thus a much more complete description is required.

Oxygen transport across the respiratory surface diffusive boundary layer is such a critical property that animals typically work to control flow and thus manage the supply of their respiratory rate needs. However there clearly are cases where the physically driven external flow field is controlling (Patterson and Sebens, 1989; Shashar et al., 1993) and is reflected in the physical distribution of organisms. And if O_2 transport is insufficient then either physical work to increase flow and thin the boundary layer is required, or organisms must resort to a temporary draw down of their finite store of alternative internal chemical energy supply.

The challenge here is in providing a useful function that more accurately describes the oceanic supply potential so as to separate as best as possible the purely physical terms which are universally applicable such as temperature T, oxygen concentration $[O_2]$, hydrostatic pressure P (together resulting in an oxygen partial pressure pO_2), diffusivity, and the basic fluid dynamical form of the dependence of boundary thickness on flow, from those properties that are unique to any one animal such as the size of the respiratory surface area and any unique characteristics of basic shape or mode of swimming or pumping.

There is no debate over combining the T, $[O_2]$, P, and diffusivity terms since these are fundamental properties. The difficulty is in providing a better way of including the flow term as a general principle. There is no doubt of the existence of a diffusive

BGD
9, 13817–13856, 2012

boundary layer that is present at all ocean surfaces, and formal descriptions of this are essential for air-sea gas exchange rates, mineral dissolution rates, and phytoplankton nutrient uptake rates. And in cases where the dimensions of the organism exceed about 1 mm (e.g. Zeebe and Wolf-Gladrow, 2001) the relationship between flow rate and boundary layer thickness is found to be strongly non-linear. The most widely used formulation is based on the dimensionless Schmidt number (e.g. Santschi et al., 1991; Wanninkhof, 1992) and this relationship is standard within the ocean sciences. There are other concepts of larger scale attached water volumes to swimming marine animals (Katija and Dabiri, 2009); these affect the bulk fluid flow properties and thus indirectly boundary layer thickness.

As the base case we use a planar surface model for the molecular exchange surface; although considerable fine structure exists the same basic diffusion rates hold. And while the animal will maintain a boundary layer typical for its respiratory needs, the physical forcing required to change the thickness of this layer will follow the same physical laws. We derive all gas flux properties on a per square centimeter scale so as to provide a way to normalize for different respiratory surface areas.

We stress that the end result of our work here cannot be profiles and maps that better describe O_2 rate limits for all organisms since individual requirements vary enormously. Rather it is the provision of relative profiles and maps that in very much the same way that profiles and maps of simple O_2 concentration values are used today can illuminate which regions of the ocean are better able to support aerobic marine life. And to do so in a more quantitative manner that permits incorporation of changes associated with ocean warming and differentiation with depth and temperature.

BGD
9, 13817–13856, 2012

3 Materials and methods

3.1 The oceanic oxygen supply potential SP_{O_2}

Oxygen uptake or respiratory exchange rates by marine animals can be treated as a two step process. Step 1 is the diffusion of dissolved oxygen across the diffusive boundary layer (DBL) which surrounds the gas exchange tissues, whether they be cell walls of single cell organisms or the gill capillaries of large marine fishes or any animal in-between. Step 2 is the diffusion of oxygen through the tissues themselves. The rate for step 1 can be expressed using the standard representation (e.g. Santschi et al., 1991; Boudreau, 1996; Zeebe and Wolf-Gladrow, 2001) of Fick's first law, using gas partial pressures (e.g. Piiper, 1982; Feder and Burggren, 1985; Pinder and Burggren, 1986; Pinder and Feder, 1990; Maxime et al., 1990; Pelster and Burggren, 1996)

$$E_{\mathrm{DBL}} = \frac{D\rho_{\mathrm{SW}}}{L} K0' \Delta pO_2|_{\mathrm{DBL}} \quad (1)$$

where E_{DBL} is the diffusive flux of oxygen across the DBL in $\mu\mathrm{mol\,s^{-1}\,cm^{-2}}$, D is the molecular diffusion coefficient for O_2 in $\mathrm{cm^2\,s^{-1}}$, L is the thickness of the diffusive boundary layer for O_2 in cm, ρ_{SW} is the density of seawater (the in situ density of seawater ρ_{SW} is calculated according to Millero and Poisson, 1981, as implemented in Hofmann et al., 2010, in $\mathrm{kg\,cm^{-3}}$), $\Delta pO_2|_{\mathrm{DBL}}$ is the oxygen partial pressure gradient across the DBL, and $K0'$ is the "apparent" Henry's Law constant in $\mu\mathrm{mol\,kg^{-1}\,matm^{-1}}$.

Here we define the "apparent" Henry's Law constant $K0'$ as the fraction of a given oxygen concentration over its associated oxygen partial pressure at given conditions, including the hydrostatic pressure dependency according to Enns et al. (1965), in contrast to the classical Henry's Law constant definition which does not include this dependency.

$$K0' = \frac{[O_2]}{pO_2([O_2], T, S, P)} \quad (2)$$

BGD
9, 13817–13856, 2012

$[O_2]$ in $\mu mol\,kg^{-1}$ is the oxygen concentration in equilibrium with pO_2, the associated oxygen partial pressure in matm calculated conventionally with the oxygen saturation concentration (Garcia and Gordon, 1992), using potential temperature (Bryden, 1973; Fofonoff, 1977), and then corrected for hydrostatic pressure P according to (Enns et al., 1965), using P values as calculated from given depth values (Fofonoff and Millard, 1983). Saturation water vapor partial pressure is accounted for as given in Zeebe and Wolf-Gladrow (2001).

The rate for step 2 of the respiratory oxygen uptake can be expressed in a similar fashion

$$E_{\text{tissue}} = \frac{D_{\text{tissue}}\rho_{\text{SW}}}{L_{\text{tissue}}}\beta\Delta pO_2|_{\text{tissue}} \tag{3}$$

where D_{tissue} is the oxygen diffusion coefficient in the tissue, L_{tissue} is the tissue thickness, β is the capacitance for O_2 transfer inside the gas exchange tissue, $\Delta pO_2|_{\text{tissue}}$ is the oxygen partial pressure gradient across the gas exchange tissue, and ρ_{SW} is the density of seawater as defined above.

The time for the transfer of a unit mass of oxygen in each step is the inverse of the diffusion rate: $t_{\text{DBL}} = \frac{1}{E_{\text{DBL}}}$ and $t_{\text{tissue}} = \frac{1}{E_{\text{tissue}}}$; thus the total time t for the transfer of a unit mass of oxygen into an animal is $t = t_{\text{DBL}} + t_{\text{tissue}}$. By inverting this expression we can write the rate equation for the complete process as

$$E = 1 \Big/ \left(\frac{1}{E_{\text{DBL}}} + \frac{1}{E_{\text{tissue}}}\right) \tag{4}$$

Our aim is to calculate the external physical constraints on respiratory gas exchange imposed by the oceanic conditions around the organism, the "oceanic oxygen supply potential". Therefore, we assume the oxygen transfer across the DBL to be the limiting step, i.e. $E_{\text{tissue}} \gg E_{\text{DBL}}$. This implies that the total oxygen flux E approaches E_{DBL}. And because the oxygen partial pressure difference across the DBL and through the gas exchange tissue is always smaller (equality in Eq. 5 would only hold in the theoretical

BGD
9, 13817–13856, 2012

limit case of the pO_2 in the venous blood being zero) than the free ocean oxygen partial pressure $pO_2|_f$, we can re-write Eq. (4) as

$$E \leq \frac{D\rho_{SW}K0'}{L} pO_2|_f \quad (5)$$

Equation (5) expresses the fact that the true respiratory gas exchange per unit area of gas exchange surface is always smaller than $\frac{D\rho_{SW}K0'}{L} pO_2|_f$. This expression, however, contains the DBL thickness L, which is an organism specific quantity as it depends on the unique size of the respiratory surface area and any unique characteristics of the organism shape and mode of swimming or pumping. So, in order to arrive at a purely physico-chemical quantity that describes the organism-independent oceanic propensity for supplying oxygen, we multiply Eq. (5) by L and arrive at

$$EL \leq D\rho_{SW}K0'pO_2|_f \quad (6)$$

This allows us to define the oceanic oxygen supply potential SP_{O_2} in $\mu mol\,s^{-1}\,cm^{-1}$ as the upper limit (i.e. maximal value) for the product of the respiratory oxygen uptake rate E and the DBL thickness L.

$$SP_{O_2} := D\rho_{SW}K0'pO_2|_f = D\rho_{SW}[O_2]_f \quad (7)$$

Thus, SP_{O_2} is a purely oceanic property, not dependent on any organism-specific properties or characteristics. It can be used to generate profiles and maps that illuminate which regions of the ocean are better able to support aerobic marine life than can simple concentration profiles or maps.

3.2 The generic maximal theoretical oxygen supply rate E_{max}

Although the DBL thickness L is organism-specific, in macroscopic organisms (in microscopic organisms, L is usually taken do be equal to the radius of the sphere of the

BGD
9, 13817–13856, 2012

microorganism (cf. e.g. Stolper et al., 2010) – in this case, our formulation for E_{max} can still be used with the appropriate L), there is a dependency of L on the fluid flow across gas exchange tissues. This flow will be some combination of the local current velocity and active pumping or swimming by the animal in question. Here, we do not aim to exactly describe the DBL thickness L for any particular animal, but we want to introduce and investigate the general dependency of L on fluid flow to compare various oceanic regions to one another as well as to have a rough measure for the energy, in terms of required flow changes, that might be required to mitigate the effects of global change such as deoxygenation, acidification and warming. To this end, we use a simple planar surface description of the flow dependency of L, as was used to describe the mineral dissolution experiments in Santschi et al. (1991). This yields the generic dependency of L on the fluid flow rate across the interface. (If one desires the organism specific dependency of L, then equations accounting for the fluid flow around the organism must be included in the derivation. This is beyond the scope of this paper.) The DBL thickness L can be expressed as the fraction of the molecular diffusion coefficient D and the mass transfer coefficient K, which is a function of the fluid flow u_{100}.

$$L = \frac{D}{K(u_{100})} \tag{8}$$

which effectively makes L a function of flow velocity u_{100}. Table 1 details this generic description of L as a function of u_{100}. Substituting Eq. (8) into Eq. (5) allows us to define an upper limit or "outer envelope" for the oxygen uptake rate E as

$$E_{max} := \frac{SP_{O_2}}{L} = \frac{D\rho_{SW}K0'}{L} pO_2|_f = K(u_{100})\rho_{SW}K0'pO_2|_f \tag{9}$$

effectively replacing the dependency on D with the dependency on the transfer coefficient K (see e.g. Santschi et al., 1991), which includes a description of the boundary layer thickness. However, it is important to note here, that we define E_{max} in Eq. (9) as $\frac{SP_{O_2}}{L}$, which makes our definition of E_{max} generic as it allows any description of the DBL

BGD
9, 13817–13856, 2012

thickness L, even a fixed, constant value, while maintaining the important dependency of E_{max} on diffusivity. As mentioned before, the definition of E_{max} as upper limit for the oxygen uptake rate as defined in Eq. (9), utilizes a simplified and generic model to describe L. E_{max} values are thus not specific to any particular animal, but are intended solely to compare various oceanic regions in their potential to support aerobic life and in their potential for resilience against global change. At the same time, values of SP_{O_2} can be converted to an organism specific upper limit for oxygen uptake by dividing by an organism specific boundary layer thickness L and considering the area of the gas exchange surface of the organism in question.

3.3 The minimal oxygen concentration C_f supporting a given, laboratory-determined E

In order to explicitly describe and reveal the influence of temperature and diffusion while comparing various oceanic regions, warm and shallow, as well as deep and cold to one another, we define another quantity in which we remove the effect of the oxygen content of the water. To explicitly include the important dependence of gas exchange on partial pressure (e.g. Piiper, 1982; Pinder and Feder, 1990; Pelster and Burggren, 1996; Childress and Seibel, 1998; Seibel et al., 1999) and the dependency of partial pressure on hydrostatic pressure (Enns et al., 1965), we assume a given oxygen uptake rate E (in $\mu mol\,s^{-1}\,cm^{-2}$), experimentally determined at diffusivities D and DBL thicknesses L equal to the respective in-situ values, but at one atmosphere. From Eq. (5) we can then determine a relation between the free stream oxygen partial pressure $pO_2|_f$ and this given oxygen uptake rate E as

$$pO_2|_f \geq \frac{L}{D\rho_{SW}K0'_E}E \tag{10}$$

which expresses that $pO_2|_f$ has to be larger or equal to the right hand side of Eq. (10) to support the given E. Again describing a limiting condition, we define p_f as the minimal

BGD
9, 13817–13856, 2012

$pO_2|_f$ that can support E as

$$p_f := \frac{L}{D\rho_{SW}K0'_E}E \tag{11}$$

As mentioned above, we assume experimental conditions at one atmosphere, so the apparent Henry's Law constant $K0'_E$ in Eqs. (10) and (11) is calculated with one atmosphere. To explicitly include the hydrostatic pressure dependency of partial pressure, i.e. to obtain the oxygen concentration that would result in p_f at in-situ hydrostatic pressures, we have to convert p_f to a concentration using an apparent Henry's Law constant $K0'_{IS}$ calculated at in-situ hydrostatic pressure. Thus, we can define C_f, the minimum oxygen concentration $[O_2]$ in $\mu mol\,kg^{-1}$ the free flowing stream must have to sustain E as

$$C_f := p_f K0'_{IS} = \frac{L}{D\rho_{SW}}\frac{K0'_{IS}}{K0'_E}E \tag{12}$$

Note that, in Eq. (12), we retain D and L as independent quantities and do not combine the two parameters to the transfer coefficient K. We do this to provide the opportunity to plug in organism specific values for L. Additionally, the inclusion of the ratio of the Henry's Law constants at one atmosphere and at in-situ pressures explicitly includes the pressure dependency of partial pressures, which makes C_f a quantity that can be used to directly compare warm and shallow to cold and deep oceanic regions.

Exemplary metabolic rates are needed to calculate reasonable examples for external O_2 limit values for a given metabolic rate, i.e. C_f values using Eq. (12). To obtain example C_f values of the appropriate scale, we choose three example oxygen uptake rates, expressed in $\mu mol\,O_2\,s^{-1}\,cm^{-2}$, that are roughly consistent with reported values for marine eggs (e.g. Yasumasu and Nakano, 1963), larvae (e.g. Houde and Schekter, 1983), embryos (e.g. Walsh et al., 1989) and adult animals (e.g. Seibel et al., 1999). If no other data was given, the given values of E were converted to per area of exchange

BGD
9, 13817–13856, 2012

surface values using a standard fish egg representation of a sphere of 1 mm diameter (Chambers and Leggett, 1996). All values have been standardized to a metabolic activity at 5 °C using a $Q10$ value of 2.5 (van Maaren, 1999). All oxygen uptake values employed are simply examples of the appropriate scale used to illustrate the calculation and use of the C_f values defined here. These examples are chosen solely to illustrate the introduced generally applicable physical concept of C_f over a range of physically realistic values.

3.4 The theoretically required flow velocity change to offset warming and deoxygenation scenarios Δu_{100}

Ocean warming not only often increases metabolic demand in animals (i.e. their required E values increase), but it also influences the physical environment that the ocean provides for aerobic life, here expressed as E_{max}. To determine the hospitability of certain ocean regions under ocean warming scenarios, changed E values have to be compared to changed E_{max} values. How E values change with temperature, i.e. how metabolic demand rises with temperature, is very organism specific and is beyond the scope of this paper. Here we focus on the effect of ocean warming on E_{max}, a measure for the physical environment that the ocean provides for aerobic life.

E_{max} is influenced by ocean warming in two major ways. Warming enhances diffusion and increases pO_2 for a given $[O_2]$, both of which increases E_{max} for otherwise constant conditions. However, warming also entails a decrease in oxygen concentration due to the temperature dependency of oxygen solubility, resulting in a decrease of $[O_2]$ which decreases E_{max}. To investigate which effect is dominant and to characterize the physical requirements for offsetting change, i.e. to maintain the same E_{max} values, we calculated the fluid flow velocity change required to offset ocean warming and resulting deoxygenation scenarios of 1 °C, 2 °C, and 3 °C. To this end, we define a quantity that expresses the required flow change under a given warming and deoxygenation

BGD
9, 13817–13856, 2012

scenario as

$$\Delta u_{100} := u_{100}^{\Delta T, E_{\max}=\mathrm{ct}} - u_{100}^{\mathrm{base}} \tag{13}$$

with u_{100}^{base} being the canonical mean background flow value of $2\,\mathrm{cm\,s^{-1}}$ used throughout this paper (also used as the typical flow rate across the gill surface in Hughes, 1966) and $u_{100}^{\Delta T, E_{\max}=\mathrm{ct}}$ being the bulk fluid flow value that results under changed conditions (ΔT and resulting $\Delta[O_2]$) in the same $E_{\max}$ value as $u_{100} = u_{100}^{\mathrm{base}}$ under standard T, $[O_2]$ conditions. $u_{100}^{\Delta T, E_{\max}=\mathrm{ct}}$ is calculated with a numercial root finding procedure using Eq. (9). This is done by first calculating $E_{\max}$ for unchanged conditions and then numerically finding the fluid flow value that yields that same $E_{\max}$ under an assumed change in T and $[O_2]$, i.e. finding the root of the function

$$0 \stackrel{!}{=} \left| E_{\max}\left(T, [O_2], u_{100}^{\mathrm{base}}\right) - E_{\max}\left(T + \Delta T, [O_2] - \Delta[O_2], u_{100}^{\Delta T, E_{\max}=\mathrm{ct}}\right) \right| \tag{14}$$

with $u_{100}^{\Delta T, E_{\max}=\mathrm{ct}}$ being the variable. Although we are aware that it will take a considerable amount of time for temperature changes be manifested in the whole ocean, for the sake of simplicity and to illustrate the concept, we use a constant temperature offset at all depths in the watercolumn for plots and tables of Δu_{100}. We note that pronounced ocean warming (Nakanowatari et al., 2007; Lyman et al., 2010) and O_2 depletion (Stramma et al., 2008) has already been observed in the upper 1 km. Oxygen concentration offsets are calculated from temperature dependent solubility changes based on in situ base temperatures.

3.5 Example oceanographic data

All T, S, P, and $[O_2]$ data for ocean profiles have been extracted from the Ocean Data View (Schlitzer, 2010) version of the World-Ocean-Atlas 2009 oxygen climatology (Garcia et al., 2010). Calculations have been performed in the open-source programming language R (R Development Core Team, 2010).

BGD
9, 13817–13856, 2012

4 Results and discussion

As noted above, warming of the ocean (Levitus et al., 2005; Lyman et al., 2010) is reducing the oxygen concentration via the solubility effect, decreasing ventilation and increasing oxygen drawdown from microbial mineralization of organic matter. Thus global ocean oxygen concentrations are declining (Chen et al., 1999; Jenkins, 2008; Stramma et al., 2008), and the combined effects of T and O_2 have impact on aerobic performance (Poertner and Knust, 2007). Yet at the same time, increased temperature enhances diffusion, and results in increased gas partial pressures for the same concentrations, both of which enhance diffusive oxygen uptake rates. The properties we define above allow for a comparison of the relative roles and impacts of these changing oceanic properties.

To illustrate our newly defined quantities, we have chosen a set of example stations from different ocean basins for comparative purposes. Table 2 provides a tabulation for the classical oxygen concentration ($[O_2]$) hydrographic depth profiles as well as depth profiles of all quantities defined in this paper, calculated with data from the World-Ocean-Atlas 2009 (Garcia et al., 2010) oxygen climatolygy for six example stations around the world ocean and the Mediterranean (SC: Southern California (120.5° W, 29.5° N); WP: Western Pacific (126.5° E, 11.5° N); CH: Chile (75.5° W, 33.5° S); WA: Western Africa (6.5° E, 15.5° S); BB: Bay of Bengal (87.5° E, 18.5° N); MD: Mediterranean (18.5° E, 35.5° N)).

4.1 Describing the oxygen supply potential of the ocean including temperature effects: $[O_2]$ vs. SP_{O_2}

The leftmost column per station in Table 2 and Fig. 1 show classical oxygen concentration profiles and the second column in Table 2 and Fig. 2 show depth profiles of our newly defined oxygen supply potential SP_{O_2} (Eq. 7). It can be clearly seen that, while the general shape of the profiles is similar due to the dominating oxygen signal, there are marked differences especially at depth.

BGD
9, 13817–13856, 2012

Those differences can be attributed to the effect of temperature dependent diffusivity that is included in the definition of SP_{O_2}. For example, while the oxygen concentration increases again to about 60 % of surface values at 4000 m depth for the three Pacific Ocean stations shown (left panel, Fig. 1), SP_{O_2} values (left panel, Fig. 2) increase only to about 40 % of surface values due to colder temperatures limiting diffusion at depth. Similarly, the right panels of Figs. 1 and 2 show that, while the oxygen concentration at the West-Africa station rises above Mediterranean values at a depth of about 1500 m (Fig. 1), SP_{O_2} values remain higher in the Mediterranean all the way down to 4000 m depth (Fig. 2) due to diffusivity-enhancing higher temperatures. In the profiles shown for the station off Chile (CH, left panels of Figs. 1 and 2), the well known horizontal penetration of an oxygen maximum into the oxygen minimum zone (Wyrtki, 1962) is reflected in the calculated SP_{O_2} values, however, the local maximum is less pronounced for SP_{O_2} than for $[O_2]$ due to the effect of temperature. The sample station in the Mediterranean (MD, right panels of Figs. 1 and 2), where there is a combination of the least diffusive restriction due to higher temperatures and a mean oxygen concentration being nearly twice as high as the site examined off Southern California (212 vs. 114 $\mu mol\,kg^{-1}$), results in the highest deep water oxygen supply potential (SP_{O_2}) values for locations we have examined. At the Bay of Bengal station (BB, right panel of Fig. 2), the waters at 800 m and below have a higher oxygen supply potential than the Southern California (SC) station, but at shallower depths the situation is reversed.

4.2 Incorporating a generic description of the influence of fluid flow velocity on gas exchange: E_{max}

The quantity E_{max} (Eq. 9, Fig. 3, third column per station in table 2) determines the combined influences of oxygen concentration, temperature, and fluid flow velocity over gas exchange surfaces, so as to provide an estimate of the maximal diffusive transport rates per unit gas exchange area that the ocean can support. Using a canonical constant current velocity of $u_{100} = 2\,cm\,s^{-1}$ we can visualize example profiles of our quantity E_{max} at our example stations in the world oceans (Fig. 3), which are, due to

BGD
9, 13817–13856, 2012

the constant u_{100}, very similar in shape to the SP_{O_2} profiles in Fig. 2. To calculate E_{max} values and profiles for specific purposes, detailed flow fields and organism-specific descriptions for the DBL thickness L should be used or more specific molecular exchange models employed (see, e.g. Lazier and Mann, 1989; Karp-Boss et al., 1996). Here, we define E_{max} with a generic description of its dependency on L and thus fluid flow velocity u_{100} to be able to define the quantity Δu_{100} to estimate the relative energy requirement needed to mitigate certain ocean warming and deoxygenation scenarios, as will be discussed in Sect. 4.4.

While being simplified, the description for the DBL thickness implemented here reproduces the general non-linear dependency of L on the fluid flow velocity u_{100}, and the dependency of this relation on temperature (leftmost panel in Fig. 4). Although for real animals, considerable fine structure of gas exchange tissues may exist, and the animal will maintain a boundary layer typical for its respiratory needs, the physical forcing required to change the thickness of this layer will follow the same physical laws. While equivalently one could plot the mass transfer coefficient K, we plot the DBL thickness L here (similar to Santschi et al., 1991), as it can be better visualized and intuitively understood. K however, is equivalent to the "gas transfer velocity" or "piston velocity" commonly used to describe air-sea gas exchange, both for the open ocean (Wanninkhof, 1992) and coastal seas (e.g. Gypens et al., 2004) and estuaries (Hofmann et al., 2008), so the underlying simplified physical formalism is the same. The limit case of $u_{100} \rightarrow 0$ would yield $L \rightarrow \infty$. This example formulation for L (or better K) as a function of u_{100} is thus not defined in a physically meaningful way for zero flow velocity and should not be used for the stagnant water case. Here we plot L with a minimum of $u_{100} = 0.5\,\mathrm{cm\,s^{-1}}$, which can be seen as an operational lower limit.

4.3 Revealing the influences of temperature, flow, and hydrostatic pressure on gas exchange: C_f

To explicitly single out the influence of temperature and fluid flow on gas exchange, which is co-mingled with the oxygen signal in profiles of SP_{O_2} and E_{max}, and to

BGD
9, 13817–13856, 2012

additionally incorporate the effect of hydrostatic pressure when comparing various oceanic regions in their ability to support given laboratory-determined respiratory rates E, we have defined the quantity C_f. C_f profiles can then be compared to $[O_2]$ profiles to determine oceanic regions that support the given oxygen demand E.

Due to the nonlinear dependency of the thickness of the diffusive boundary layer L on the current velocity u_{100}, the minimal oxygen concentration C_f supporting a given oxygen uptake rate E is also a nonlinear function of u_{100}. The middle panel of Fig. 4 explicitly visualizes this dependency for different temperatures but constant pressure and salinity, and the right panel of Fig. 4 depicts this dependency for different hydrostatic pressures. The left panel of Fig. 5 shows depth profiles of C_f for the Southern California (SC) example hydrographical station (i.e. with in-situ temperature, salinity and pressure) for three different values for u_{100}. This further illustrates the sensitivity of C_f with respect to u_{100}.

It can be shown for the range of u_{100} values in the middle panel of Fig. 4, that a u_{100} decrease by half results in approximately a doubling of C_f (i.e. C_f is roughly proportional to the inverse of u_{100}). The nonlinear character of the relation between the fluid flow velocity u_{100} and the limit free stream oxygen concentration C_f is such that there is a low dependency when when $u_{100} > 2\,\mathrm{cm\,s^{-1}}$ and very high dependency when $u_{100} < 1\,\mathrm{cm\,s^{-1}}$. This is a result of the respective behavior of the thickness of the diffusive boundary layer L on u_{100}, as also described by e.g. Garmo et al. (2006).

The right panel of Fig. 5 shows example depth profiles of C_f at the SC station for three different respiratory rates E, on realistic orders of magnitude, to express the sensitivity of C_f with respect to E.

The general shape of C_f depth profiles in Fig. 5 can be explained by comparison of C_f (Eq. 12) with its direct predecessor quantity p_f (Eq. 11), the minimal oxygen partial pressure required to support E. The quantity C_f directly includes effects of diffusivity, boundary layer thickness, and temperature and hydrostatic pressure effects on partial pressure. The predecessor quantity p_f expresses only effects on diffusivity and boundary layer thickness. As temperature decreases with depth, so does the "efficiency" of

BGD
9, 13817–13856, 2012

diffusion, with the result that L increases. This translates into a higher p_f with depth, i.e. a higher necessary pO_2 to sustain the given oxygen consumption rate E. The limit oxygen concentration C_f initially follows suit, but as hydrostatic pressure increases with depth, so does the pO_2 for a given $[O_2]$ (Enns et al., 1965). This means that p_f, the pO_2 necessary to sustain E, which is more or less constant with depth from below 2000 m, as temperature does not change anymore, is sustained by a smaller and smaller oxygen concentration: C_f decreases from about 2000 m on.

Different ocean basins exhibit markedly different temperature and salinity profiles; these differences affect the quantity C_f since this subsumes the influences of temperature, salinity and hydrostatic pressure on diffusive gas transport. Figure 6 and the fourth column in Table 2 show C_f depth profiles for our example hydrographical stations, assuming a constant current velocity of $2\,cm\,s^{-1}$. In the Pacific, the profiles are rather similar, while warm enclosed seas like the Mediterranean differ markedly. Here, due to warm temperatures throughout the water column, the entire profiles are shifted towards lower C_f values. It is remarkable that in the Mediterranean, the oxygen concentration at 4000 m depth required to sustain a given oxygen consumption rate is lower than at the surface. In the Atlantic the C_f maximum is sharply defined at around 1000 m depth; in the Pacific the maximum is more broadly defined at around the same depth, in keeping with classical hydrographic profiles. In the Indian Ocean (Bay of Bengal), the C_f maximum is deeper at $\approx$ 2000 m. Given the marked similarity of C_f profiles in the Pacific (left panel of Fig. 6), one can conclude that the differences in oxygen supply potential SP_{O_2} between various stations in the Pacific (left panel of Fig. 2) are mainly due to differences in oxygen concentration profiles. This is not the case for the example stations that are not located in the Pacific (right panels of Figs. 2 and 6), where the effects of temperature and pressure considerably contribute to the differences in SP_{O_2} profiles.

Even though our exact description of the dependency is generalized, the fact that the limit oxygen concentration C_f is dependent on current velocity makes it necessary that water flow rates be included in the set of variables that are controlled or reported when

BGD
9, 13817–13856, 2012

comparing different systems or different animal responses (e.g. Stachowitsch et al., 2007; Riedel et al., 2008; Haselmair et al., 2010). This dependency also indicates that sessile benthic animals in high current environments have an advantage in low oxygen conditions over free swimming fish and over zooplankton that are suspended relatively stationary with respect to the water mass surrounding it. It also explains why under the same low oxygen conditions, continental slopes or the flanks of seamounts experiencing comparatively high mixing rates and currents (van Haren and Gostiaux, 2010) can be more hospitable environments for animals than comparatively stagnant waters.

4.4 First-order estimate of the energy required for mitigation of global change scenarios: Δu_{100}

In order to investigate which of the multiple effects of warming and deoxygenation will be dominant for certain locations in the ocean, we define the quantity Δu_{100}; this describes the flow offset from the canonical value of $2\,\mathrm{cm\,s^{-1}}$ needed to keep $E_{\max}$ constant under global warming and deoxygenation scenarios. It is essentially the work that must be done to thin the boundary layer so as to restore a required O_2 uptake rate.

For a first order estimate we assume that the oxygen concentration decreases for a given constant temperature offset by only the difference in the oxygen saturation concentration at every location in the profile. We are aware that this will underestimate true ocean changes, as increased T will also result in higher microbial oxygen consumption rates fueled by the large mass of organic carbon stored in ocean organic matter in sediments, seawater, and sinking particles. Figure 7 and the fifth to seventh columns in Table 2 show Δu_{100} values for all our example stations and 1 °C, 2 °C, and 3 °C warming scenarios.

It can be seen that within the oxygen minimum zone, especially off the Southern California (SC) and the Bay of Bengal (BB) locations, a relatively high flow increase would be needed to compensate for the warming and deoxygenation scenario. As the oxygen concentration becomes small, very high flow rates are necessary to adequately

BGD
9, 13817–13856, 2012

decrease L and thus to maintain E_{max} at its original value. The reason for this is the rather flat dependency of diffusive transport on flow for flow values higher than 2 cm s^{-1} (see Fig. 4). These then will clearly be very highly stressed regions under even modest ocean warming scenarios.

In marked contrast in warm regions at depths shallower than the oxygen minimum zone and particularly in the warm Mediterranean Sea, the diffusion enhancement of increased temperatures overcompensates for the oxygen concentration loss. Thus Δu_{100} values are negative, which means a flow less than 2 cm s^{-1} would suffice to provide the same E_{max} as in the base case. But recall that we assume here only a solubility reduction in [O_2] and in practice Δ[O_2] will be significantly higher.

The effect is principally due to the fact that the solubility, and thus the oxygen concentration difference, is smaller for warm waters than it is for cold waters and thus temperature enhanced diffusion overcomes the effect of deoxygenation. The absolute values of negative Δu_{100} flow rates are smaller than the positive ones since the relationship of L with flow is much steeper as flow rates decrease below 2 cm s^{-1} (see Fig. 4).

The estimates provided here are of the physico-chemical properties for inter-regional comparison and actual impacts will be species specific. Furthermore, we are only investigating the effect of ocean warming on the oceanic supply of oxygen. The effect of increased temperature on the oxygen demand, i.e. the increased metabolic demand of the organism now living at higher temperature, which presumably is very organism specific, is not treated here.

5 Summary and conclusions

In this publication we define quantities that describe the ocean's ability to supply oxygen, based on diffusive boundary transport rate limitations. These quantities subsume well known oceanic physical properties relevant to diffusive boundary transport into functions that may be used for various purposes.

BGD
9, 13817–13856, 2012

The oxygen supply potential SP_{O_2} and the maximal oxygen supply rate E_{max} an environment can sustain are the more general parameters that could be used to map specific oceanic regions according to their ability to supply oxygen. The limit oxygen concentration C_f supporting a given demand rate E is the quantity that explicitly expresses the effects of tempertature, flow and hydrostatic pressure, without the obstruction by the oxygen concentration signal. C_f values can be used to roughly estimate the hospitability of certain regions for particular animals with known oxygen uptake rate requirements. We also define the quantity Δu_{100} that describes the significance of ocean warming and deoxygenation scenarios to aerobic life by specifying the flow offset necessary to counteract the presented scenarios. In cases with adverse effects to animals, the required increase in flow as expressed by positive Δu_{100} values is an indicator of the physical energy required to maintain the same maximal oxygen supply rate (E_{max}). Whether this required energy will be supplied by the energy contained in ambient flow or is a result of animal activity like pumping or swimming is deliberately not distinguished here.

All our newly defined quantities express the requirements and limitations imposed only by the oceanic physical environment. The results from example oceanographic stations around the world strongly suggest a greater diversity of regions and a more complex response of biogeochemical cycles to ocean warming than anticipated from the simple change in O_2 concentration alone. It should not be surprising that the fields produced appear superficially to resemble traditional O_2 concentration profiles and maps; descriptions of the formation of the [O_2] minimum and well established gradients along major ocean circulation pathways are dominant features and powerful drivers that have long been described (Wyrtki, 1962). It is for this reason that the relatively crude representation of various limits by simple concentration values has been in use for so long; they are familiar and have served as reasonable approximations. But the basic kinetic rate representation given here allows for much greater insight, in particular for different oceanic depth realms and for an ocean changing simultaneously in T and [O_2]. For example the basic solubility equation always results in lower O_2 concentration from

BGD
9, 13817–13856, 2012

ocean warming, which may be interpreted as more limiting to aerobic life. But when combined with the essential temperature and pressure dependencies of pO_2 and diffusivity, a more complex picture emerges.

Acknowledgements. This work was supported by a grant to the Monterey Bay Aquarium Research Institute from the David and Lucile Packard Foundation.

References

Biron, P. M., Robson, C., Lapointe, M. F., and Gaskin, S. J.: Comparing different methods of bed shear stress estimates in simple and complex flow fields, Earth Surf. Proc. Land., 29, 1403–1415, doi:10.1002/esp.1111, 2004. 13846

Boudreau, B. P.: Diagenetic Models and Their Implementation, Springer, Berlin, 1996. 13823, 13846

Bryden, H. L.: New polynomials for thermal expansion, adiabatic temperature gradient and potential temperature of sea water, Deep-Sea Res., 20, 401–408, 1973. 13824

Chambers, R. C. and Leggett, W. C.: Maternal influences on variation in egg sizes in temperate marine fishes, Am. Zool., 36, 180–196, doi:10.1093/icb/36.2.180, 1996. 13829

Chen, C. T. A., Bychkov, A. S., Wang, S. L., and Pavlova, G. Y.: An anoxic Sea of Japan by the year 2200?, Mar. Chem., 67, 249–265, 1999. 13831

Childress, J. J. and Seibel, B. A.: Life at stable low oxygen levels: adaptations of animals to oceanic oxygen minimum layers, J. Exp. Biol., 201, 1223–1232, 1998. 13827

Ekau, W., Auel, H., Pörtner, H.-O., and Gilbert, D.: Impacts of hypoxia on the structure and processes in pelagic communities (zooplankton, macro-invertebrates and fish), Biogeosciences, 7, 1669–1699, doi:10.5194/bg-7-1669-2010, 2010. 13819

Enns, T., Scholander, P. F., and Bradstreet, E. D.: Effect of hydrostatic pressure on gases dissolved in water, J. Phys. Chem., 69, 389–391, 1965. 13823, 13824, 13827, 13835

Feder, M. E. and Burggren, W. W.: Cutaneous gas exchange in vertebrates: design, patterns, control and implications., Biol. Rev. Camb. Philos. Soc., 60, 1–45, 1985. 13823

Fofonoff, N. P.: Computation of potential temperature of seawater for an arbitrary reference pressure, Deep-Sea Res., 24, 489–491, 1977. 13824

BGD

9, 13817–13856, 2012

Fofonoff, N. P. and Millard, R. C. J.: Algorithms for computation of fundamental properties of seawater, UNESCO technical papers in marine science, 44, 55 pp., 1983. 13824
Garcia, H. E. and Gordon, L. I.: Oxygen solubility in seawater – better fitting equations, Limnol. Oceanogr., 37, 1307–1312, 1992. 13819, 13824
Garcia, H. E., Locarnini, R. A., Boyer, T. P., Antonov, J. I., Baranova, O. K., Zweng, M. M., and Johnson, D. R.: World Ocean Atlas 2009, Volume 3: Dissolved Oxygen, Apparent Oxygen Utilization, and Oxygen Saturation, NOAA Atlas NESDIS 70, edited by: Levitus, S., US Government Printing Office, Washington DC, 344 pp., 2010. 13830, 13831
Garmo, O., Naqvi, K., Royset, O., and Steinnes, E.: Estimation of diffusive boundary layer thickness in studies involving diffusive gradients in thin films (DGT), Anal. Bioanal. Chem., 386, 2233–2237, doi:10.1007/s00216-006-0885-4, 2006. 13834
Gilbert, D., Rabalais, N. N., Díaz, R. J., and Zhang, J.: Evidence for greater oxygen decline rates in the coastal ocean than in the open ocean, Biogeosciences, 7, 2283–2296, doi:10.5194/bg-7-2283-2010, 2010. 13819
Gooday, A. J., Jorissen, F., Levin, L. A., Middelburg, J. J., Naqvi, S. W. A., Rabalais, N. N., Scranton, M., and Zhang, J.: Historical records of coastal eutrophication-induced hypoxia, Biogeosciences, 6, 1707–1745, doi:10.5194/bg-6-1707-2009, 2009. 13819
Gray, J. S., Shiu-sun, R., and Or, Y. Y.: Effects of hypoxia and organic enrichment on the coastal marine environment, Mar. Ecol.-Prog. Ser., 238, 249–279, 2002. 13819
Gypens, N., Lancelot, C., and Borges, A. V.: Carbon dynamics and CO_2 air–sea exchanges in the eutrophied coastal waters of the Southern Bight of the North Sea: a modelling study, Biogeosciences, 1, 147–157, doi:10.5194/bg-1-147-2004, 2004. 13833
Haselmair, A., Stachowitsch, M., Zuschin, M., and Riedel, B.: Behaviour and mortality of benthic crustaceans in response to experimentally induced hypoxia and anoxia in situ, Mar. Ecol.-Prog. Ser., 414, 195–208, 2010. 13836
Hickey, B., Baker, E., and Kachel, N.: Suspended particle movement in and around Quinault submarine canyon, Mar. Geol., 71, 35–83, doi:10.1016/0025-3227(86)90032-0, 1986. 13846
Hofmann, A. F., Soetaert, K., and Middelburg, J. J.: Present nitrogen and carbon dynamics in the Scheldt estuary using a novel 1-D model, Biogeosciences, 5, 981–1006, doi:10.5194/bg-5-981-2008, 2008. 13833
Hofmann, A. F., Soetaert, K., Middelburg, J. J., and Meysman, F. J. R.: AquaEnv: an aquatic acid-base modelling environment in R, Aquat. Geochem., 16, 507–546, 2010. 13823

BGD
9, 13817–13856, 2012

Hofmann, A. F., Peltzer, E. T., Walz, P. M., and Brewer, P. G.: Hypoxia by degrees: establishing definitions for a changing ocean, Deep-Sea Res. Pt. I, 58, 1212–1226, doi:10.1016/j.dsr.2011.09.004, 2011. 13821

Houde, E. D. and Schekter, R. C.: Oxygen uptake and comparative energetics among eggs and larvae of three subtropical marine fishes, Mar. Biol., 72, 283–293, doi:10.1007/BF00396834, 1983. 13828

Hughes, G. M.: The dimensions of fish gills in relation to their function, J. Exp. Biol., 45, 177–195, 1966. 13820, 13830

Jenkins, W. J.: The biogeochemical consequences of changing ventilation in the Japan/East Sea, Mar. Chem., 108, 137–147, doi:10.1016/j.marchem.2007.11.003, 2008. 13831

Karp-Boss, L., Boss, E., and Jumars, P.: Nutrient fluxes to planktonic osmotrophs in the presence of fluid motion, Oceanogr. Mar. Biol. Ann. Rev., 34, 71–107, 1996. 13820, 13833

Katija, K. and Dabiri, J. O.: A viscosity-enhanced mechanism for biogenic ocean mixing, Nature, 460, 624–626, doi:10.1038/nature08207, 2009. 13822

Kemp, W. M., Testa, J. M., Conley, D. J., Gilbert, D., and Hagy, J. D.: Temporal responses of coastal hypoxia to nutrient loading and physical controls, Biogeosciences, 6, 2985–3008, doi:10.5194/bg-6-2985-2009, 2009. 13819

Lazier, J. R. N. and Mann, K. H.: Turbulence and diffusive layers around small organisms, Deep-Sea Res. Pt. I, 36, 1721–1733, 1989. 13820, 13833

Levin, L. A., Ekau, W., Gooday, A. J., Jorissen, F., Middelburg, J. J., Naqvi, S. W. A., Neira, C., Rabalais, N. N., and Zhang, J.: Effects of natural and human-induced hypoxia on coastal benthos, Biogeosciences, 6, 2063–2098, doi:10.5194/bg-6-2063-2009, 2009. 13819

Levitus, S., Antonov, J., and Boyer, T. P.: Warming of the world ocean, Geophys. Res. Lett., 32, 1955–2003, 2005. 13831

Lyman, J. M., Good, S. A., Gouretski, V. V., Ishii, M., Johnson, G. C., Palmer, M. D., Smith, D. M., and Willis, J. K.: Robust warming of the global upper ocean, Nature, 465, 334–337, 2010. 13830, 13831

Maxime, V., Peyraud-Waitzenegger, M., Claireaux, G., and Peyraud, C.: Effects of rapid transfer from sea water to fresh water on respiratory variables, blood acid-base status and O_2 affinity of haemoglobin in Atlantic salmon (*Salmo salar* L.), J. Comp. Physiol. B, 160, 31–39, 1990. 13823

Middelburg, J. J. and Levin, L. A.: Coastal hypoxia and sediment biogeochemistry, Biogeosciences, 6, 1273–1293, doi:10.5194/bg-6-1273-2009, 2009. 13819

BGD

9, 13817–13856, 2012

Millero, F. J. and Poisson, A.: International one-atmosphere equation of state of seawater, Deep-Sea Res. Pt. I, 28, 625–629, 1981. 13823
Nakanowatari, T., Ohshima, K. I., and Wakatsuchi, M.: Warming and oxygen decrease of intermediate water in the Northwestern North Pacific, originating from the Sea of Okhotsk, 1955–2004, Geophys. Res. Lett., 34, L04602, doi:10.1029/2006GL028243, 2007. 13830
Naqvi, S. W. A., Bange, H. W., Farías, L., Monteiro, P. M. S., Scranton, M. I., and Zhang, J.: Marine hypoxia/anoxia as a source of CH_4 and N_2O, Biogeosciences, 7, 2159–2190, doi:10.5194/bg-7-2159-2010, 2010. 13819
Palumbi, S. R., Sandifer, P. A., Allan, J. D., Beck, M. W., Fautin, D. G., Fogarty, M. J., Halpern, B. S., Incze, L. S., Leong, J.-A., Norse, E., Stachowicz, J. J., and Wall, D. H.: Managing for ocean biodiversity to sustain marine ecosystem services, Front. Ecol. Environ., 7, 204–211, doi:10.1890/070135, 2009. 13820
Patterson, M. R. and Sebens, K. P.: Forced-convection modulates gas-exchange in Cnidarians, Proc. Natl. Acad. Sci. USA, 86, 8833–8836, doi:10.1073/pnas.86.22.8833, 1989. 13821
Pelster, B. and Burggren, W. W.: Disruption of hemoglobin oxygen transport does not impact oxygen-dependent physiological processes in developing embryos of zebra fish (*Danio rerio*), Circ. Res., 79, 358–362, 1996. 13823, 13827
Peña, M. A., Katsev, S., Oguz, T., and Gilbert, D.: Modeling dissolved oxygen dynamics and hypoxia, Biogeosciences, 7, 933–957, doi:10.5194/bg-7-933-2010, 2010. 13819
Piiper, J.: Respiratory gas exchange at lungs, gills and tissues: mechanisms and adjustments, J. Exp. Biol., 100, 5–22, 1982. 13823, 13827
Pinczewski, W. V. and Sideman, S.: A model for mass (heat) transfer in turbulent tube flow, Moderate and high Schmidt (Prandtl) numbers, Chem. Eng. Sci., 29, 1969–1976, doi:10.1016/0009-2509(74)85016-5, 1974. 13846
Pinder, A. W. and Burggren, W. W.: Ventilation and partitioning of oxygen uptake in the frog rana pipiens: effects of hypoxia and activity, J. Exp. Biol., 126, 453–468, 1986. 13823
Pinder, A. W. and Feder, M. E.: Effect of boundary layers on cutaneous gas exchange, J. Exp. Biol., 154, 67–80, 1990. 13823, 13827
Poertner, H. O. and Knust, R.: Climate change affects marine fishes through the oxygen limitation of thermal tolerance, Science, 315, 95–97, doi:10.1126/science.1135471, 2007. 13831
R Development Core Team: R: A Language and Environment for Statistical Computing, R Foundation for Statistical Computing, Vienna, Austria, available at: http://www.R-project.org, 2010. 13830

BGD
9, 13817–13856, 2012

Rabalais, N. N., Díaz, R. J., Levin, L. A., Turner, R. E., Gilbert, D., and Zhang, J.: Dynamics and distribution of natural and human-caused hypoxia, Biogeosciences, 7, 585–619, doi:10.5194/bg-7-585-2010, 2010. 13819

Riedel, B., Zuschin, M., Haselmair, A., and Stachowitsch, M.: Oxygen depletion under glass: behavioural responses of benthic macrofauna to induced anoxia in the Northern Adriatic, J. Exp. Mar. Biol. Ecol., 367, 17–27, doi:10.1016/j.jembe.2008.08.007, 2008. 13836

Santschi, P. H., Anderson, R. F., Fleisher, M. Q., and Bowles, W.: Measurements of diffusive sublayer thicknesses in the ocean by alabaster dissolution, and their implications for the measurements of benthic fluxes, J. Geophys. Res., 96, 10641–10657, doi:10.1029/91JC00488, 1991. 13822, 13823, 13826, 13833, 13846

Schlitzer, R.: Ocean Data View 4, available at: http://odv.awi.de, 2010. 13830

Seibel, B. A., Chausson, F., Lallier, F. H., Zal, F., and Childress, J. J.: Vampire blood: respiratory physiology of the vampire squid (*Cephalopoda*: *Vampyromorpha*) in relation to the oxygen minimum layer, Exp. Biol. Online, 4, 1–10, doi:10.1007/s00898-999-0001-2, 1999. 13827, 13828

Shaffer, G., Olsen, S. M., and Pedersen, J. O. P.: Long-term ocean oxygen depletion in response to carbon dioxide emissions from fossil fuels, Nat. Geosci., 2, 105–109, doi:10.1038/NGEO420, 2009. 13819

Shashar, N., Cohen, Y., and Loya, Y.: Extreme diel fluctuations of oxygen in diffusive boundary-layers surrounding stony corals, Biol. Bullet., 185, 455–461, 1993. 13821

Shaw, D. A. and Hanratty, T. J.: Turbulent mass transfer rates to a wall for large Schmidt numbers, AICHE J., 23, 28–37, doi:10.1002/aic.690230106, 1977. 13846

Soetaert, K., Petzoldt, T., and Meysman, F.: Marelac: tools for aquatic sciences, available at: http://CRAN.R-project.org/package=marelac, r package version 2.1, 2010. 13846

Stachowitsch, M., Riedel, B., Zuschin, M., and Machan, R.: Oxygen depletion and benthic mortalities: the first in situ experimental approach to documenting an elusive phenomenon, Limnol. Oceanogr.-Methods, 5, 344–352, 2007. 13836

Sternberg, R. W.: Friction factors in tidal channels with differing bed roughness, Mar. Geol., 6, 243–260, doi:10.1016/0025-3227(68)90033-9, 1968. 13846

Stolper, D. A., Revsbech, N. P., and Canfield, D. E.: Aerobic growth at nanomolar oxygen concentrations, Proc. Natl. Acad. Sci. USA, 107, 18755–18760, 2010. 13826

Stramma, L., Johnson, G. C., Sprintall, J., and Mohrholz, V.: Expanding oxygen-minimum zones in the tropical oceans, Science, 320, 655–658, 2008. 13830, 13831

BGD

9, 13817–13856, 2012

Tallis, H., Lester, S. E., Ruckelshaus, M., Plummer, M., McLeod, K., Guerry, A., Andelman, S., Caldwell, M. R., Conte, M., Copps, S., Fox, D., Fujita, R., Gaines, S. D., Gelfenbaum, G., Gold, B., Kareiva, P., ki Kim, C., Lee, K., Papenfus, M., Redman, S., Silliman, B., Wainger, L., and White, C.: New metrics for managing and sustaining the ocean's bounty, Mar. Policy, 36, 303–306, doi:10.1016/j.marpol.2011.03.013, 2012. 13820

van Haren, H. and Gostiaux, L.: A deep-ocean Kelvin–Helmholtz billow train, Geophys. Res. Lett., 37, L03605, doi:10.1029/2009GL041890, 2010. 13836

van Maaren, C. C., Kita, J., and Daniels, H. V.: Temperature tolerance and oxygen consumption rates for juvenile southern flounder *paralichthys lethostigma* acclimated to five different temperatures, UJNR Technical Report No. 28, 135–140, available at: http://www.lib.noaa.gov/retiredsites/japan/aquaculture/proceedings.htm, 1999. 13829

Walsh, W. A., Swanson, C., Lee, C.-S., Banno, J. E., and Eda, H.: Oxygen consumption by eggs and larvae of striped mullet, *Mugil cephalus*, in relation to development, salinity and temperature, J. Fish Biol., 35, 347–358, doi:10.1111/j.1095-8649.1989.tb02987.x, 1989. 13828

Wanninkhof, R.: Relationship between wind-speed and gas-exchange over the ocean, J. Geophys. Res.-Oceans, 97, 7373–7382, 1992. 13821, 13822, 13833, 13846

Weiss, R. F.: Solubility of nitrogen, oxygen and argon in water and seawater, Deep-Sea Res., 17, 721–735, 1970. 13819

Weiss, R. F.: Carbon dioxide in water and seawater: the solubility of a non-ideal gas, Mar. Chem., 2, 203–215, 1974. 13819

Wood, P. E. and Petty, C. A.: New model for turbulent mass transfer near a rigid interface, AICHE J., 29, 164–167, doi:10.1002/aic.690290126, 1983. 13846

Wyrtki, K.: The oxygen minima in relation to ocean circulation, Deep-Sea Res., 9, 11–23, 1962. 13832, 13838

Yasumasu, I. and Nakano, E.: Respiratory level of sea urchin eggs before and after fertilization, Biol. Bullet., 125, 182–187, 1963. 13828

Zeebe, R. E. and Wolf-Gladrow, D.: CO_2 in Seawater: Equilibrium, Kinetics, Isotopes, no. 65 in Elsevier Oceanography Series, Elsevier, first edn., Amsterdam, 2001. 13822, 13823, 13824

Zhang, J., Gilbert, D., Gooday, A. J., Levin, L., Naqvi, S. W. A., Middelburg, J. J., Scranton, M., Ekau, W., Peña, A., Dewitte, B., Oguz, T., Monteiro, P. M. S., Urban, E., Rabalais, N. N., Ittekkot, V., Kemp, W. M., Ulloa, O., Elmgren, R., Escobar-Briones, E., and Van der Plas, A. K.: Natural and human-induced hypoxia and consequences for coastal

BGD
9, 13817–13856, 2012

areas: synthesis and future development, Biogeosciences, 7, 1443–1467, doi:10.5194/bg-7-1443-2010, 2010. 13819

BGD
9, 13817–13856, 2012

Table 1. Expressing the DBL thickness L as a function of water flow velocity: a generic planar surface description.

The DBL thickness L can be expressed as the fraction of the temperature-dependent molecular diffusion coefficient D for O_2 in $cm^2 s^{-1}$, calculated from temperature and salinity as given in Boudreau (1996, Chapter 4) using the implementation in the *R* package marelac (Soetaert et al., 2010), and the mass transfer coefficient K (Santschi et al., 1991; Boudreau, 1996)

$$L = \frac{D}{K} \tag{15}$$

K can be calculated for O_2 from the water-flow induced shear velocity u' in $cm\,s^{-1}$ and the dimensionless Schmidt number Sc for O_2 (as calculated by linearly interpolating two temperature dependent formulations for $S = 35$ and $S = 0$ in Wanninkhof, 1992, with respect to given salinity)

$$K = au'\mathrm{Sc}^{-b} \tag{16}$$

with parameters a and b: Santschi et al. (1991): $a = 0.078$, $b = \frac{2}{3}$; Shaw and Hanratty (1977) (also given in Boudreau, 1996, $a = 0.0889$, $b = 0.704$); Pinczewski and Sideman (1974) as given in Boudreau (1996): $a = 0.0671$, $b = \frac{2}{3}$; Wood and Petty (1983) as given in Boudreau (1996): $a = 0.0967$, $b = \frac{7}{10}$. Due to small differences we use averaged results of all formulations.
u' can be calculated from the ambient current velocity at 100 cm away from the exchange surface u_{100} and the dimensionless drag coefficient c_{100} (Sternberg, 1968; Santschi et al., 1991; Biron et al., 2004)

$$u' = u_{100}\sqrt{c_{100}} \tag{17}$$

c_{100} is calculated from the water flow velocity u_{100} as (Hickey et al., 1986; Santschi et al., 1991)

$$c_{100} = 10^{-3}(2.33 - 0.0526|u_{100}| + 0.000365|u_{100}|^2) \tag{18}$$

BGD
9, 13817–13856, 2012

Table 2. Depth profiles of $[O_2]$, SP_{O_2}, E_{max}, C_f, Δu_{100} for example stations around the world. Details on the tabulated quantities can be found in the text. Δu_{100} values are calculated for three ocean warming and associated deoxygenation scenarios (1 °C, 2 °C, 3 °C). The units used are: $[O_2]$: $\mu mol\,kg^{-1}$; SP_{O_2}: $10^{-7}\,\mu mol\,kg^{-1}\,s^{-1}\,cm^{-1}$; E_{max}: $10^{-7}\,\mu mol\,kg^{-1}\,s^{-1}\,cm^{-2}$; C_f: $\mu mol\,kg^{-1}$; Δu_{100}: $cm\,s^{-1}$. For all locations we assume a constant flow velocity of $u_{100} = 2\,cm\,s^{-1}$, more realistic flow profiles or organism specific descriptions of the DBL thickness L can be employed here. $T_E = 5$ °C and $S_E = 34$. NA indicates that values are not available for the respective depth, Inf indicates situations where Δu_{100} is not defined since subtracting the saturation concentration difference associated with the temperature increase from the actual oxygen concentration would result in negative oxygen concentrations. SC: Southern California (120.5° W, 29.5° N); WP: Western Pacific (126.5° E, 11.5° N); CH: Chile (75.5° W, 33.5° S); WA: Western Africa (6.5° E, 15.5° S); BB: Bay of Bengal (87.5° E, 18.5° N); MD: Mediterranean (18.5° E, 35.5° N).

depth	$[O_2]$	SP_{O_2}	E_{max}	C_f	Δu_{100} 1 °C	Δu_{100} 2 °C	Δu_{100} 3 °C
SC							
0	239	46	221	16.72	−0.032	−0.062	−0.091
50	246	46	218	17.80	−0.034	−0.066	−0.096
100	230	40	183	20.75	−0.033	−0.063	−0.092
200	143	22	96	26.41	0.002	0.005	0.010
300	85	13	54	28.57	0.072	0.156	0.252
400	44	6	26	30.17	0.265	0.631	1.169
500	23	3	13	31.27	0.758	2.580	13.136
600	16	2	9	32.06	1.514	15.523	Inf
700	15	2	9	32.62	1.652	28.285	Inf
800	18	3	10	33.07	1.229	7.126	Inf
900	22	3	12	33.35	0.877	3.332	70.135
1000	28	4	15	33.63	0.636	1.958	6.370
1100	32	4	17	33.81	0.526	1.490	3.820
1200	36	5	19	33.90	0.442	1.181	2.659
1300	41	6	21	33.95	0.359	0.907	1.845
1400	46	6	24	33.97	0.305	0.745	1.432
1500	53	7	27	33.93	0.253	0.599	1.097
2000	82	11	40	33.37	0.124	0.272	0.451
3000	118	15	56	29.99	0.057	0.121	0.193
4000	132	17	63	26.22	0.041	0.085	0.135
WP							
0	225	46	227	14.73	−0.030	−0.060	−0.090
50	235	44	211	17.46	−0.033	−0.065	−0.095
100	226	41	192	18.81	−0.033	−0.064	−0.093
200	211	37	176	19.14	−0.030	−0.059	−0.085
300	202	36	167	19.20	−0.028	−0.055	−0.080
400	199	35	162	19.20	−0.028	−0.053	−0.077
500	193	34	157	19.15	−0.026	−0.051	−0.073
600	188	33	152	19.05	−0.025	−0.048	−0.069
700	187	33	151	18.90	−0.025	−0.047	−0.068
800	184	32	148	18.72	−0.024	−0.046	−0.066
900	185	32	148	18.53	−0.024	−0.046	−0.067
1000	185	32	148	18.33	−0.024	−0.046	−0.066
1100	186	32	149	18.11	−0.024	−0.047	−0.068

BGD
9, 13817–13856, 2012

Table 2. Continued.

depth	$[O_2]$	SP_{O_2}	E_{max}	C_f	Δu_{100} 1 °C	Δu_{100} 2 °C	Δu_{100} 3 °C
WP							
1200	190	33	152	17.88	−0.025	−0.049	−0.071
1300	185	32	148	17.66	−0.024	−0.046	−0.066
1400	190	33	152	17.44	−0.025	−0.049	−0.071
1500	181	31	144	17.20	−0.023	−0.043	−0.062
2000	192	33	153	16.11	−0.026	−0.050	−0.072
3000	183	32	147	14.06	−0.023	−0.045	−0.065
4000	190	33	152	12.29	−0.025	−0.049	−0.070
CH							
0	196	48	262	9.76	−0.052	−0.111	−0.181
50	200	49	264	9.88	−0.050	−0.107	−0.172
100	198	46	245	10.73	−0.038	−0.081	−0.129
200	176	33	161	16.66	−0.019	−0.036	−0.052
300	135	22	98	23.22	0.002	0.007	0.014
400	91	14	58	27.35	0.058	0.125	0.201
500	78	11	47	29.65	0.092	0.200	0.328
600	90	13	52	30.65	0.073	0.156	0.252
700	96	14	55	31.46	0.065	0.139	0.223
800	94	13	53	31.92	0.071	0.152	0.245
900	92	13	50	32.50	0.078	0.168	0.272
1000	94	13	51	32.79	0.076	0.163	0.264
1100	96	13	51	33.18	0.075	0.161	0.260
1200	94	13	50	33.38	0.080	0.172	0.279
1300	101	14	52	33.61	0.071	0.151	0.243
1400	102	14	52	33.76	0.070	0.150	0.241
1500	108	14	55	33.73	0.063	0.134	0.215
2000	115	15	57	33.02	0.057	0.120	0.191
3000	142	18	68	30.11	0.031	0.065	0.103
4000	152	20	72	26.27	0.023	0.047	0.074
WA							
0	245	45	214	18.29	−0.034	−0.066	−0.097
50	230	41	191	19.59	−0.032	−0.063	−0.091
100	185	31	139	22.56	−0.021	−0.041	−0.059
200	76	12	53	24.91	0.077	0.166	0.270
300	46	7	30	26.79	0.215	0.497	0.884
400	91	13	56	29.19	0.063	0.135	0.218
500	157	23	92	31.23	0.001	0.002	0.006
600	195	27	110	32.34	−0.015	−0.030	−0.044
700	184	26	102	33.03	−0.009	−0.018	−0.027
800	154	21	84	33.44	0.008	0.017	0.028
900	134	18	72	33.89	0.025	0.053	0.085
1000	123	17	65	34.11	0.038	0.081	0.129
1100	114	15	59	34.21	0.051	0.107	0.171
1200	112	15	58	34.20	0.054	0.115	0.184
1300	110	15	56	34.18	0.058	0.122	0.195
1400	112	15	57	34.13	0.057	0.120	0.191
1500	115	15	58	34.04	0.054	0.114	0.181
2000	134	17	66	33.06	0.035	0.073	0.115
3000	152	20	73	29.64	0.021	0.044	0.069
4000	169	22	81	26.04	0.010	0.021	0.033

BGD
9, 13817–13856, 2012

Table 2. Continued.

depth	$[O_2]$	SP_{O_2}	E_{max}	C_f	Δu_{100} 1 °C	Δu_{100} 2 °C	Δu_{100} 3 °C
BB							
0	222	46	233	13.88	−0.030	−0.059	−0.089
50	169	33	160	16.10	−0.017	−0.033	−0.048
100	80	14	65	20.05	0.053	0.114	0.183
200	58	10	43	22.73	0.120	0.265	0.440
300	40	6	28	24.94	0.249	0.587	1.073
400	45	7	29	27.19	0.226	0.525	0.943
500	60	9	37	29.24	0.151	0.338	0.574
600	78	11	45	30.98	0.099	0.216	0.354
700	96	14	54	32.19	0.066	0.142	0.228
800	120	17	65	33.06	0.037	0.078	0.124
900	135	18	72	33.53	0.024	0.050	0.080
1000	146	20	78	33.62	0.016	0.033	0.053
1100	153	21	81	33.48	0.011	0.024	0.038
1200	166	22	87	33.22	0.003	0.007	0.013
1300	175	24	92	32.87	−0.002	−0.003	−0.003
1400	188	25	98	32.52	−0.008	−0.015	−0.022
1500	199	27	104	32.17	−0.013	−0.025	−0.037
2000	220	30	113	30.90	−0.019	−0.038	−0.057
3000	225	30	112	28.19	−0.019	−0.038	−0.056
4000	230	30	114	24.87	−0.020	−0.040	−0.059
MD							
0	204	50	268	9.97	−0.048	−0.103	−0.167
50	165	39	207	10.66	−0.032	−0.070	−0.114
100	40	8	42	13.53	0.144	0.315	0.523
200	14	2	11	19.97	1.065	4.891	Inf
300	15	2	11	22.79	1.094	5.237	Inf
400	15	2	10	23.83	1.165	6.117	Inf
500	16	2	11	24.59	1.079	5.084	Inf
600	17	3	11	25.35	1.030	4.592	Inf
700	22	3	14	26.08	0.663	2.081	7.259
800	25	4	16	26.74	0.573	1.678	4.696
900	32	5	20	27.42	0.403	1.047	2.240
1000	40	6	24	28.09	0.299	0.728	1.392
1100	44	6	26	28.65	0.267	0.637	1.183
1200	50	7	29	29.19	0.224	0.521	0.933
1300	55	8	31	29.66	0.198	0.453	0.794
1400	67	9	37	30.16	0.146	0.324	0.547
1500	75	10	40	30.47	0.123	0.270	0.449
2000	106	14	53	32.05	0.066	0.141	0.226
3000	NA	NA	NA	NA	NA	NA	NA
4000	NA	NA	NA	NA	NA	NA	NA

BGD
9, 13817–13856, 2012

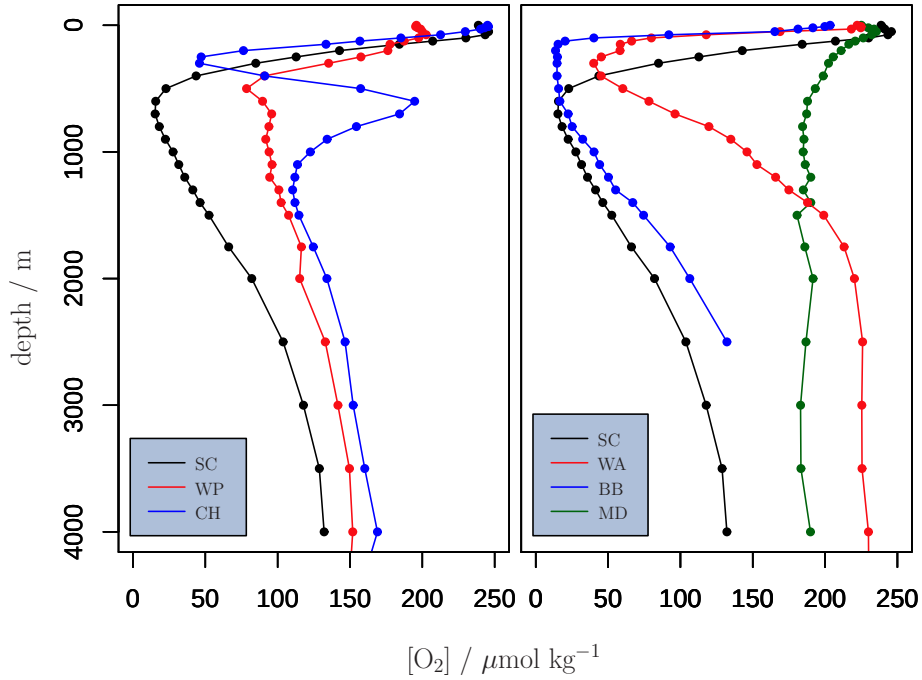

Fig. 1. [O_2] depth profiles of the water column at different hydrographical stations around the world (SC: Southern California (120.5° W, 29.5° N); CH: Chile (75.5° W, 33.5° S); WP: Western Pacific (126.5° E, 11.5° N), WA: Western Africa (6.5° E, 15.5° S), MD: Mediterranean (18.5° E, 35.5° N); BB: Bay of Bengal (87.5° E, 18.5° N)).

BGD
9, 13817–13856, 2012

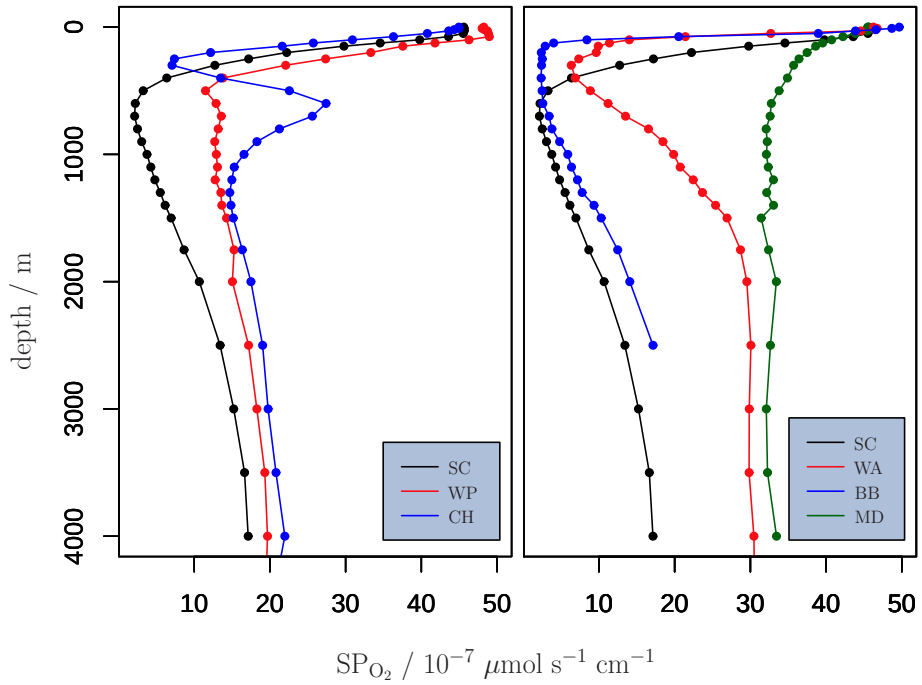

Fig. 2. Oxygen supply potential SP_{O_2} depth profiles of the water column at different hydrographical stations around the world (SC: Southern California (120.5° W, 29.5° N); CH: Chile (75.5° W, 33.5° S); WP: Western Pacific (126.5° E, 11.5° N), WA: Western Africa (6.5° E, 15.5° S), MD: Mediterranean (18.5° E, 35.5° N); BB: Bay of Bengal (87.5° E, 18.5° N)).

BGD
9, 13817–13856, 2012

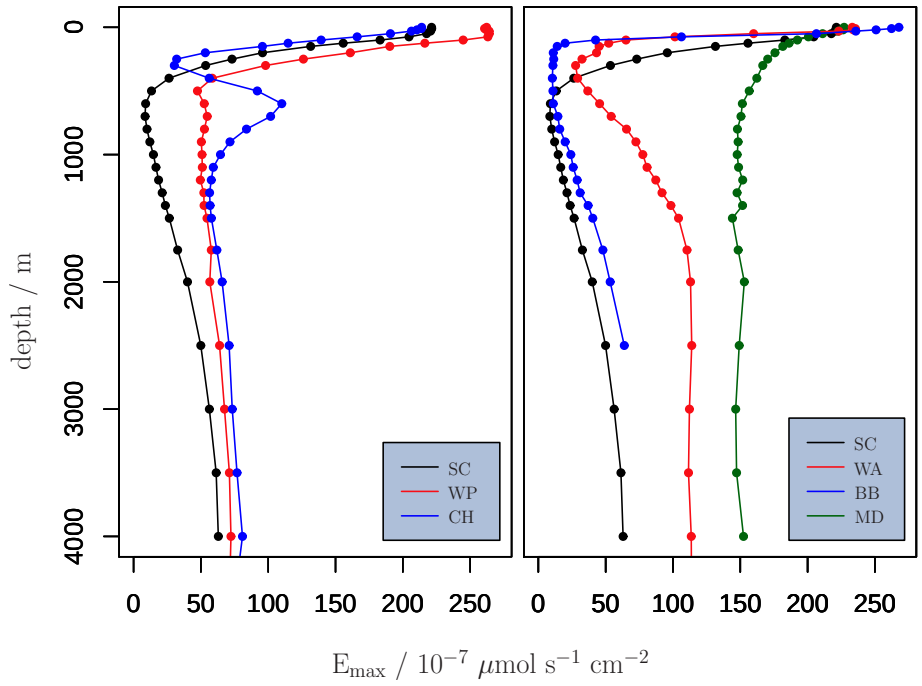

Fig. 3. Generic maximal theoretical oxygen supply rate E_{max} depth profiles of the water column at different hydrographical stations around the world (SC: Southern California (120.5° W, 29.5° N); CH: Chile (75.5° W, 33.5° S); WP: Western Pacific (126.5° E, 11.5° N), WA: Western Africa (6.5° E, 15.5° S), MD: Mediterranean (18.5° E, 35.5° N); BB: Bay of Bengal (87.5° E, 18.5° N)). A generic flow velocity of $u_{100} = 2\,\mathrm{cm\,s^{-1}}$ is assumed for all depths to calculate L. If available, detailed flow profiles can be used here, as well as organism-specific descriptions for L.

BGD
9, 13817–13856, 2012

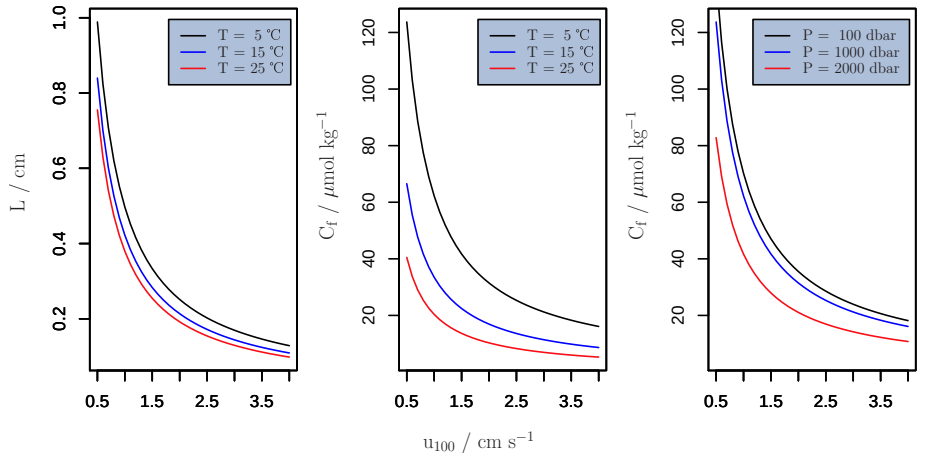

Fig. 4. The influence of flow velocity u_{100}, temperature T and hydrostatic pressure P on the DBL thickness L and C_f, the minimal oxygen concentration supporting a given, laboratory determined oxygen uptake rate E. The dependency of L (and all derived quantities) on u_{100} is based on the simple exemplary model description employed here. While individual organism-specific dependencies may vary in detail, the general dependency of L on the flow velocity is captured here. Unless stated otherwise in the legend: Latitude = 29.5° N, S = 34, T = 5 °C, P = 100 bar, $E = 20 \times 10^{-7}$ µmol s^{-1} cm^{-2}, T_E = 5 °C, and S_E = 34.

BGD
9, 13817–13856, 2012

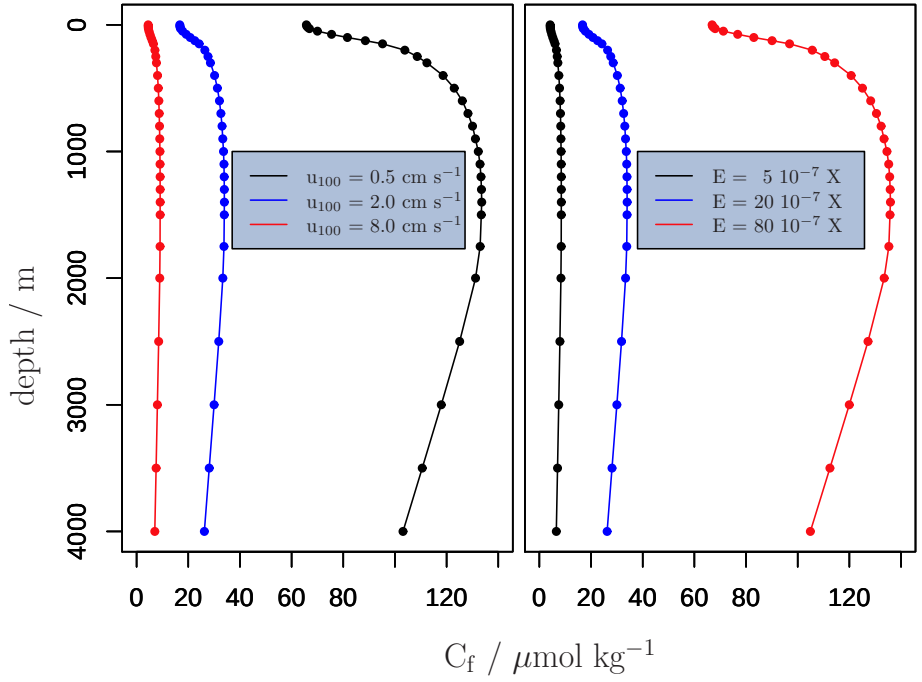

Fig. 5. The influence of flow velocity u_{100} and the given, laboratory-determined oxygen uptake rate E (X = µmol s^{-1} cm^{-2}), along depth profiles of temperature T, and hydrostatic pressure P at the Pacific station SC off Southern California (120.5° W, 29.5° N). T_E = 5 °C, and S_E = 34.

BGD
9, 13817–13856, 2012

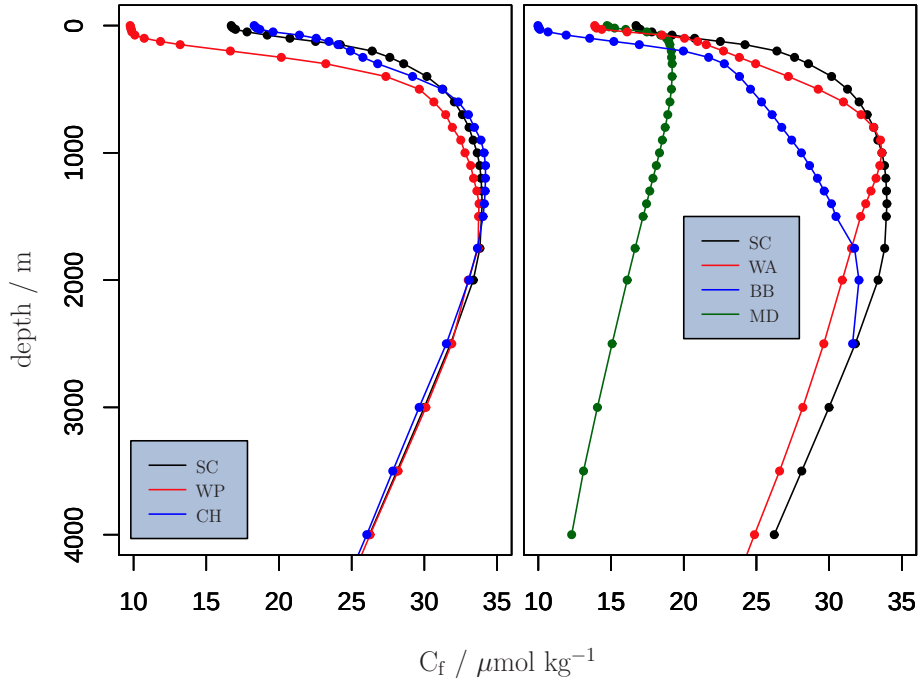

Fig. 6. Minimal oxygen concentration C_f, supporting a given, laboratory determined oxygen uptake rate, depth profiles of the water column at different hydrographical stations around the world (SC: Southern California (120.5° W, 29.5° N); CH: Chile (75.5° W, 33.5° S); WP: Western Pacific (126.5° E, 11.5° N), WA: Western Africa (6.5° E, 15.5° S), MD: Mediterranean (18.5° E, 35.5° N); BB: Bay of Bengal (87.5° E, 18.5° N)). A generic flow velocity of $u_{100} = 2\,\mathrm{cm\,s^{-1}}$ is assumed for all depths to calculate L. If available, detailed flow profiles can be used here, as well as organism-specific descriptions for L.

BGD
9, 13817–13856, 2012

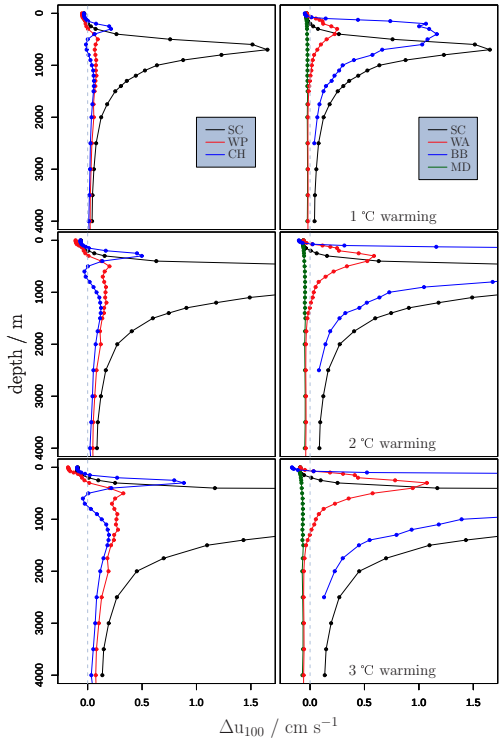

Fig. 7. Flow offset Δu_{100} that would be required to keep E_{max} constant under three ocean warming and deoxygenation scenarios (1 °C, 2 °C, 3 °C) along a set of temperature, salinity and pressure depth profiles of the water column at different hydrographical stations around the world (SC: Southern California (120.5° W, 29.5° N); CH: Chile (75.5° W, 33.5° S); WP: Western Pacific (126.5° E, 11.5° N), WA: Western Africa (6.5° E, 15.5° S), MD: Mediterranean (18.5° E, 35.5° N); BB: Bay of Bengal (87.5° E, 18.5° N)); Assumed generic base flow value: $u_{100}^{base} = 2\,cm\,s^{-1}$. At every point $[O_2]$ is assumed to decrease according to the offset in oxygen saturation concentration, using in-situ T as base value and applying the respective assumed temperature change. Positive values of Δu_{100} indicate that the flow would have to be increased from the base value of $2\,cm\,s^{-1}$ to compensate for the combined warming and deoxygenation effects, negative values indicate that a slower flow would suffice to provide the same E_{max} as in the base case. To not loose details on the small scale and to limit the plots to meaningful values, we truncated the abscissa to Δu_{100} values $\leq 1.65\,cm\,s^{-1}$.

BGD
9, 13817–13856, 2012